FULL PAPER

p-Nitrophenol Removal from Aqueous Solution Using Raw and Modified Kaolinite

Folahan Amoo Adekola[a], Sodiq Jimoh[a], and Adejumoke Abosede Inyinbor[*b]

[a]Industrial Chemistry Department, University of Ilorin, P.M.B 1515, Ilorin, Nigeria.
[b]Physical Sciences Department, Landmark University, P.M.B 1001, Omu Aran, Nigeria.

Abstract:

Natural adsorbent prepared from kaolin clay (RK) as well as RK modified separately with cysteine (CYMK), and chitosan (CHMK) was used for the removal of *p*-nitrophenol (PNP) from aqueous solution. Prepared adsorbents were fully characterized using X-ray diffraction (XRD), X-ray fluorescence (XRF), scanning electron microscope (SEM) and Fourier Transformed Infrared Spectroscopy (FTIR). Vivid characteristics of kaolinite were shown by FTIR spectroscopy and surface modification showed new absorption bands which corresponds to the unique functional groups in the modifying agents. Surface morphology was also altered after modification. Surface modification enhanced adsorption capacity. Adsorption data fitted best into the Freundlich adsorption isotherm for the three adsorption systems thus suggesting multi surface adsorption. The maximum monolayer adsorption capacities were 6.94 mg/g, 4.61 mg/g and 6.56 mg/g for PNP-RK, PNP-CYMK and PNP-CHMK systems respectively. The pseudo second order kinetics best described the kinetics of the adsorption system. Temperature effects showed that the adsorbents were stable across the temperature considered and thermodynamic parameters showed that the adsorption processes were feasible and spontaneous.

Keywords: p-nitrophenol; kaolin; chitosan; cysteine

1. Introduction

Organic pollutant is one thematic challenge of today's environment. Phenols, which has been classified as priority pollutant, has found great use in pharmaceutical, petrochemical, steel, plastic and coal industries [1]. Phenols are characterized by high toxicity to plants, aquatic organism, animals and human therefore the maximum allowable concentration in wastewater has been set to 1 mg/L. Human exposure to phenolic derivatives concentration above maximum limit may lead to damage of the organs amongst other diseases [2]. For instance, p-nitrophenol (PNP) which is used as antifungal in leather protection, pesticides, explosives and dyestuff productions causes liver and kidney damage, methemoglobin formation, anemia as well as eye and skin irritation [3]. The removal of PNP a widely utilized organic compound from industrial wastewater before their eventual discharge is therefore of utmost importance.

Several conventional methods of wastewater treatment exist and quit a number of this have been explored for PNP removal [4-9]. Simplicity and ease of operation have given adsorption preference over other methods of wastewater treatment [10]. Other characteristics, which make adsorption attractive, are adsorbent regeneration possibility and reusability of treated water for industrial processes, which uses water of low purity made [11]. Naturally, occurring materials in raw and modified forms are currently being explored as alternative for the expensive activated carbon thus adding economic advantage to adsorption [12-17]

Clays are strong adsorbent and have been used for decades. Qualities such as chemical and mechanical stability, layered structure, ready availability and low cost make them an excellent adsorbent for the prevailing environmental pollution challenge. Their adsorption potential/efficiency largely depends on surface area as well as exchange capacity [18]. Chitosan

---

[*]Corresponding author. E-mail: ✉ nyinbor.adejumoke@landmarkuniversity.edu.ng

on one hand is a natural adsorbent which is obtained via N-deacetylation of chitin. Chitosan with an exposed amino group is known to be highly effective for the adsorption of organic and inorganic pollutant [19]. Cysteine on the other hand contains reactive amino group coupled with carboxylate and thiol groups and it is known to be effective in adsorption of diverse pollutants too. Aside their suitability in metal and organic pollutant binding, cysteine is also known for its catalytic and redox properties which is facilitated by its thiol group [20]. While raw kaolin, chitosan and cysteine may have excellent capacities to adsorb PNP, various characteristics of individual materials as well as adsorptive properties can be enhanced via modification. Here we focus on enhancing the adsorptive capacity of raw kaolin via modification with cysteine and chitosan as well as creating a solid base for cysteine and chitosan thus increasing their stability and mechanical strength.

2. Results and Discussion

Characteristics of raw and modified kaolin

Mineralogy composition of raw and modified kaolin

The mineralogy composition of the raw and modified kaolin clay is reported in Table 1. This results showed a typical component of kaolin clay with SiO_2 having the highest percentage as expected. The ability of kaolinite to form intercalation compounds may have been responsible for the slight decrease in its main components after modification [21].

Table 1. Chemical Composition of Kaolin Mineral Sample by XRF.

Oxides	Percentage concentration (%)		
	RK	**CHMK**	**CYMK**
Al_2O_3	43.30	41.10	41.70
SiO_2	52.00	49.00	51.50
K_2O	0.041	ND	ND
CaO	0.214	0.28	0.353
TiO_2	1.68	2.07	2.19
V_2O_5	0.085	0.068	0.072
Cr_2O_3	0.036	0.047	0.051
MnO	0.016	0.014	0.015
Fe_2O_3	1.04	1.20	1.34
NiO	0.011	0.0091	0.0094
CuO	0.0071	0.01	0.0069
ZnO	0.068	0.011	0.007
Ga_2O_3	0.018	0.019	0.024
Ag_2O	1.40	1.59	1.62
Re_2O_7	0.055	0.073	0.13

Crystallographic characteristics of raw and modified kaolin

The Figure 1 depicts the XRD pattern of raw kaolinite and the modified forms. The XRD pattern reveals kaolinite characteristic peaks with intense peaks at 2Θ values of 12.5^0, 24.9^0, and 62.3^0. The intensity of the peaks at 19.8^0, 35.9^0, 37.7^0 and 38.4^0 were not as high as the first series of peaks. The spectrograph also shows the diffraction peaks of quarts at 2Θ values of 20.9^o, 26.7^o and 50.1^0.
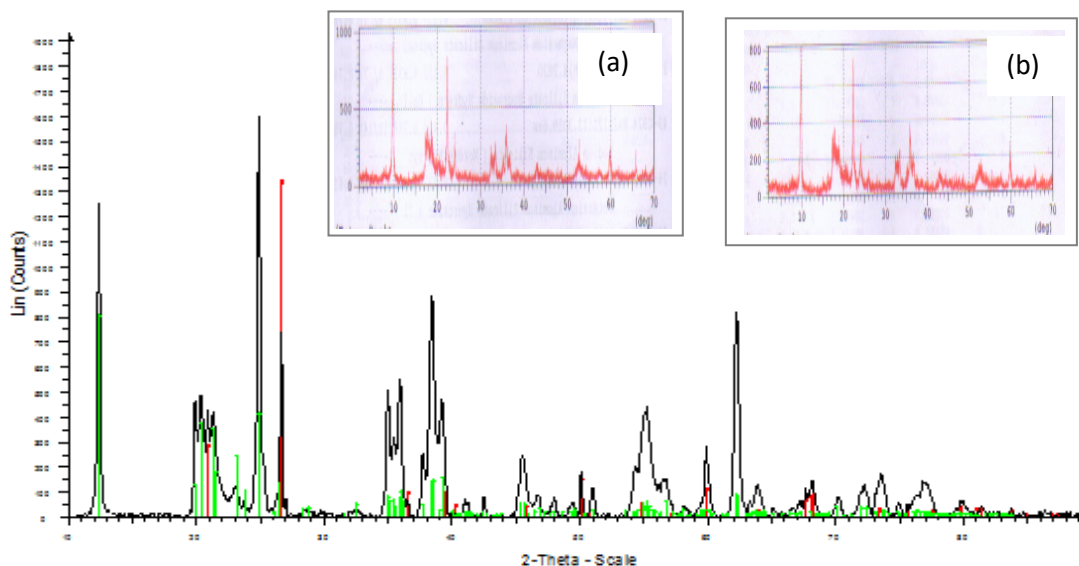

Figure 1. XRD patterns of raw kaolinite; Insert (a) XRD pattern of CHMK; (b) XRD pattern of CYMK.

Surface morphology of raw and modified kaolinite before and after PNP uptake

The SEM image of RK (Figure 2a) shows an unevenly distributed cloudlike nature with hollows and pores. Modification with cysteine (Figure 2c) results into a new morphology with various aggregates and evidenced pores. Chitosan modification (Figure 2b) however results into large aggregates with some flakes as well as hollows and tiny pores. The smooth surface earlier observed before PNP uptake (Figures 2b and 2c) was observed to have been rough after PNP uptake (Figure 2b$_1$ and 2c$_1$). Large aggregate was observed on the surface of CHMK after PNP uptake (Figure 2b$_1$).
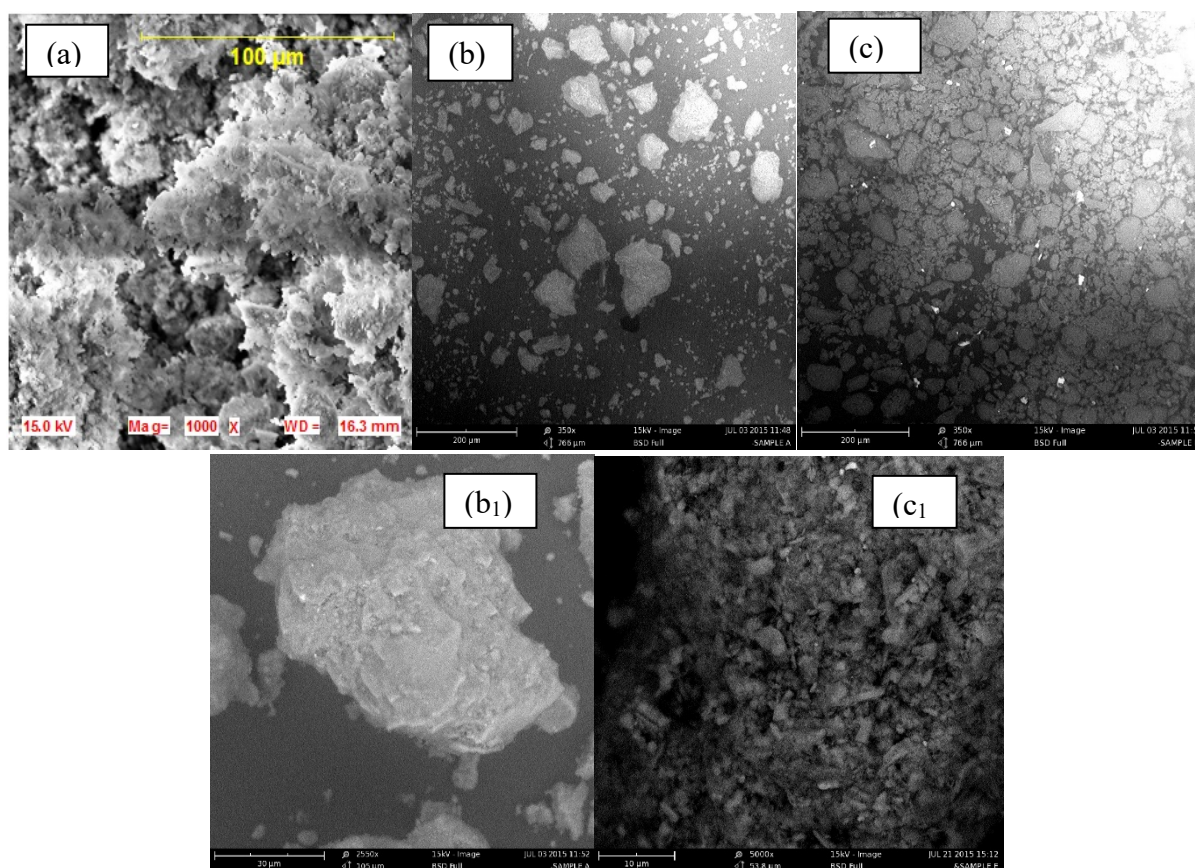

Figure 2. SEM micrograph of RK (a) CHMK (b) and CYMK (c); CHMK after PNP uptake (b$_1$) and CYMK after PNP uptake (c$_1$).

Functional group analysis of RK, CHMK and CYMK

FTIR spectra of raw kaolinite and its various modified forms before and after PNP uptake is shown in Figure 3. RK (Figure 3a) showed sharp and vivid peaks at 914 cm^{-1}, 3620 cm^{-1} and 3695 cm^{-1} which correspond to O-H bending vibration, vibration of inner –OH and stretching vibrations of surface –OH respectively. The N-H stretching vibration at 3691 cm^{-1}, vivid –OH stretching vibration of alcohol which occurred at 3442 cm^{-1}, NH$_2$ scissoring at 1639 cm^{-1}, C-N stretching vibration at 1103 cm^{-1} as well as C-O vibrations at 1022 cm^{-1} were peaks observed in CHMK (Figure 3c). A bathochromic shift of 4 cm^{-1} was observed for O-H band of RK after cysteine modification thus observed vibration at 914 cm^{-1} in RK was observed at 918 cm^{-1} in CYMK (Figure 3e). The vibrations at 1020 cm^{-1}, 1105 cm^{-1}, 2362 cm^{-1} and 3691 cm^{-1} corresponds to C-OH, C-N, S-H and O-H or N-H stretching vibrations respectively. Adsorption of ions from aqueous solution onto clay has been established to be either by ion exchange, surface complexation, hydrophobic interactions or electrostatic interactions [22]. Ion exchange as well as surface complexation was evidently displayed by great reduction in absorption bands intensity and various shift in absorption bands after PNP uptake (Figure 3b, 3d and 3f).
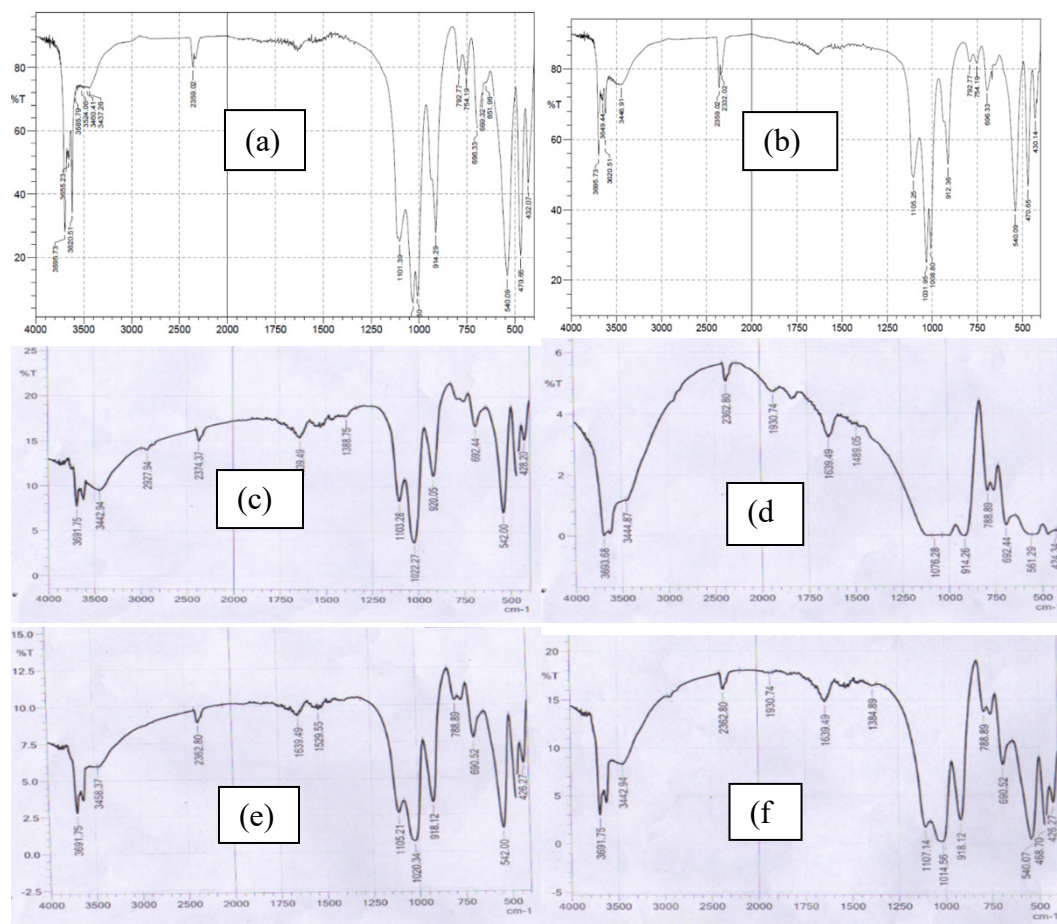
437

Orbital: Electron. J. Chem. 10 (6): 435-445, 2018

Figure 3. FTIR spectra of kaolinite clay mineral before PNP uptake (a) after PNP uptake (b); CHMK before PNP uptake (c) and after PNP uptake (d); CYMK before PNP uptake (e) and after PNP uptake (f).

Effect of initial concentration on PNP adsorption onto RK, CYMK and CHMK

Quantity of PNP adsorbed was found to increase with concentration and reached optimum at 120 mg/L (Figure 4). The initial concentration is known to provide a strong driving force for adsorbate to overcome mass transfer barrier. At concentration higher than 120 mg/L, overlap on adsorption site as well as aggregation of adsorbate may have resulted in the slight decrease observed in quantity of adsorbate uptake. Surface modification also enhanced adsorption efficiency and CHMK gave the highest performance with about 43% performance increase when compared with RK.

Effect of contact time on PNP adsorption onto RK, CYMK and CHMK

Uptake of PNP onto RK and its modified

counterpart was observed to be rapid initially, the systems gradually attained equilibrium towards 60 minutes (Figure 5). Since continuous bombardment will normally enhance adsorption, PNP uptake was observed to increase with time. Quantity of PNP removed was generally low, modification enhanced adsorption efficiency of RK. Highest quantity of PNP adsorbed by RK, CYMK and CHMK were 1.155 mg/g, 1.258 mg/g and 1.651 mg/g, respectively. Exposed adsorption sites may have been responsible for the initial rapid adsorption while percolation into pores as well as adsorbate-adsorbate interactions may have also occurred within the RK-PNP, CYMK-PNP and CHMK-PNP adsorption system [23].

Effects of pH on PNP adsorption onto RK, CYMK and CHMK

Quantity of PNP adsorbed was observed to

438

Orbital: Electron. J. Chem. 10 (6): 435-445, 2018

decrease as the pH of the solution moves from acidity to alkalinity (Figure 6). Quantity adsorbed varied between 1.16 to 0.87 mg/g, 1.26 to 1.11 mg/g and 1.65 to 1.20 mg/g for RK, CYMK and CHMK respectively across the pH considered. The ionization degree of PNP may have been responsible for the rate of its removal as the pH increased [15]. PNP exists more in its molecular form in acidic media or at pH lower than its pKa and characterized by low ionization in this media. Uptake of PNP onto the three adsorbent may have been in the molecular form rather than the phenolate ions. Mechanism of uptake may have include Van der Waal forces, hydrogen bonding and hydrophobic interactions [16, 24].
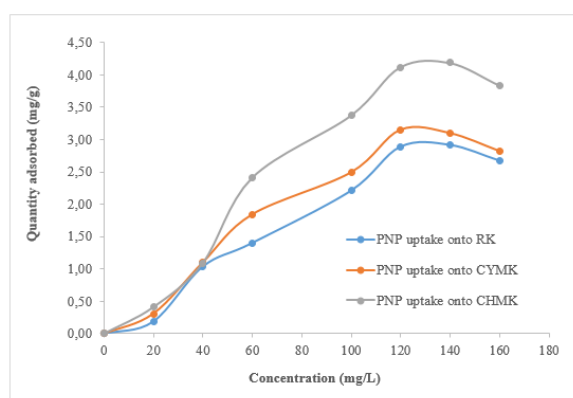
adsorbate are known to be less viscous and more mobile thus their molecules diffuses faster across the external boundary layer and in the internal pores of the adsorbent particle. The activation of adsorption sites may also occur at high temperature. In this study, changes in the uptake of PNP onto RK, and its modified counterparts as the temperature increased were negligible and tends towards insignificant decrease (Figure 7). This suggests that the prepared adsorbent were stable even at high temperature thus making it potential suitable adsorbent for industries discharging hot effluents. Changes in the arrangement of surface functional group in clay has been given as a reason for a decrease in adsorption as temperature increases [2].

Figure 4. Effects of concentration on PNP uptake onto RK, CYMK and CHMK [Adsorbent dose (2 g/L), agitation speed (130 rpm), agitation time (360 minutes), Temperature (27±2 °C), Adsorbate concentration (50 mg/L)].
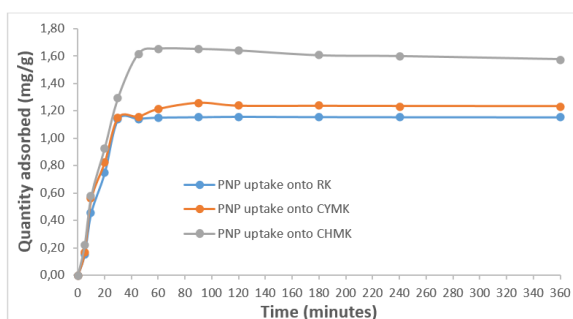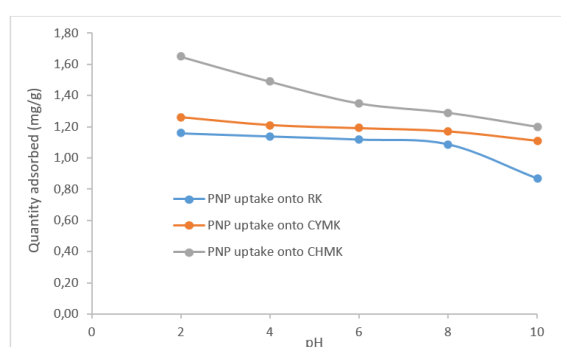

Figure 6. Effects of pH on PNP uptake onto RK, CYMK and CHMK. [Adsorbent dose (2 g/L), agitation speed (130 rpm), concentration (50 mg/L), Temperature (27±2 °C)].

Figure 5. Effects of contact time on PNP uptake onto RK, CYMK and CHMK. [Adsorbent dose (2 g/L), agitation speed (130 rpm), concentration (50 mg/L), Temperature (27±2 °C)].
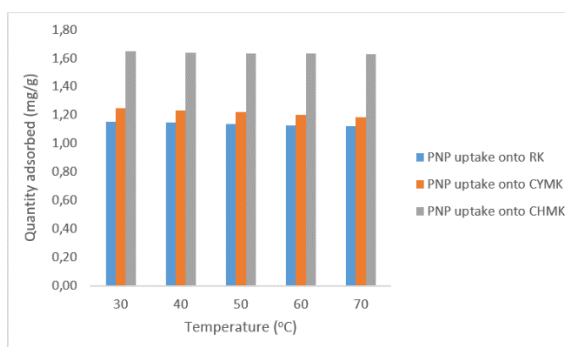
Figure 7. Effects of temperature on PNP uptake onto RK, CYMK and CHMK. [Adsorbent dose (2 g/L), agitation speed (130 rpm), concentration (120 mg/L), contact time (180 minutes, pH (2)].

Effects of temperature on PNP adsorption onto RK, CYMK and CHMK

The temperature has two major effects on the adsorption process. At higher temperature

Effect of adsorbent dosage on PNP adsorption onto RK, CYMK and CHMK

Quantity of PNP adsorbed per unit mass declined from 1.12 mg/g to 0.99 mg/g, 1.32 mg/g

439

Orbital: Electron. J. Chem. 10 (6): 435-445, 2018

to 0.99 mg/g and 1.75 mg/g to 1.08 mg/g for RK, CYMK and CHMK respectively as adsorbent dosage increased from 0.1 g to 0.5 g (Figure 8). Decrease in quantity adsorbed per unit mass as adsorbent dosage increased may be as a result of saturation of adsorption sites and particle-particle interactions leading to aggregation/agglomeration or overlap of adsorbent [16]. This reduction may also be because of variation in concentration gradient of adsorbate and adsorbent [25].

Isothermal studies of adsorption of PNP onto RK, CYMK and CHMK

Table 2 shows the isothermal parameters for PNP uptake onto the prepared adsorbents. Judging by the correlation coefficients, adsorption is predominantly to multiple surface in the three adsorption systems with adsorbate-adsorbate interaction playing a huge role in PNP removal. The maximum monolayer adsorption capacity ranged between 4.61 mg/g and 6.94 mg/g (Table

2). The R_L values, which are less than unity in all suggest that adsorption process was favourable. The value of Temkin constant b which is related to heat of adsorption were 174.42 J/mol, 162.12 J/mol and 118.47 J/mol for RK, CYMK and CHMK respectively.
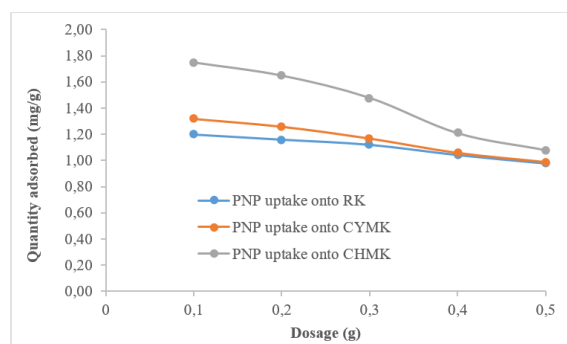

Figure 8. Effects of adsorbent dosage on PNP uptake onto RK, CYMK and CHMK. [Agitation speed (130 rpm), concentration (120 mg/L), contact time (180 minutes, pH (2), Temperature (27±2 °C)].

Table 2. Isothermal parameters for the adsorption of PNP onto RK, CYMK and CHMK.

Isotherms	constants	Adsorbents		
		RK	CYMK	CHMK
Langmuir	q_{max} (mg/g)	6.94	4.61	6.56
	K_L (L.mg^{-1})	0.0046	0.0127	0.0112
	R_L	0.5788	0.3284	0.3581
	R^2	0.8242	0.8200	0.8342
Freundlich	K_F	0.0414	0.0126	0.0124
	n	1.1443	0.8614	0.8172
	R^2	0.9867	0.9418	0.9643
Temkin	B	1.43	1.5385	2.1054
	A (L/g)	0.053	0.058	0.054
	b (J/mol)	174.42	162.12	118.47
	R^2	0.9635	0.9786	0.9593

Kinetics studies of PNP adsorption onto RK, CYMK and CHMK

The pseudo second order kinetics with correlation coefficient very close to one best describe the adsorption data of the three adsorption systems. The SSE and X^2 for the pseudo second order kinetics were also low, especially for RK-PNP and CYMK-PNP systems. The rate constant for the pseudo second order kinetics were found to be greater than that of the pseudo first order kinetic across the concentration considered. A multilinear adsorption profile was obtained for the intraparticle diffusion plot (Figure not shown), this suggests that adsorption process

were in two distinct stages thus corroborating the isothermal results which indicates predominance of a multilayer adsorption. Boundary layer diffusion may have been the first stage of the adsorption process while in the subsequent gradual sorption stage, intraparticle diffusion was the rate limiting step. The observed values for K_{diff1} are greater than values obtained for K_{diff2} (Table 3), this suggests that intraparticle diffusion mainly controls sorption rate [26].

Thermodynamic studies of PNP uptake onto RK, CYMK and CHMK

Positive values obtained for enthalpy (ΔH^o) (Table 4) for the three adsorption system indicates that the adsorption processes within these systems were endothermic in nature. ΔS^o values were also positive across the three adsorption system suggesting increase in the randomness at the solid-liquid interface within the adsorption systems. This randomness at the solid-liquid interface could result from the higher translational entropy acquired by the displaced water molecules as compared to that lost as a result of PNP uptake [27]. The spontaneity and feasibility of the adsorption process was established as negative values were obtained for ΔG^o across the studied temperature within the three systems.

Table 3. Kinetics parameters for the adsorption of PNP onto RK, CYMK and CHMK.

Constants	Adsorbents		
	RK	**CYMK**	**CHMK**
$q_{e\ experimental}$ (mg/L)	1.155	1.258	1.651
Pseudo first order			
$q_{e\ calculated}$ (mg/L)	0.843	1.199	2.923
$K_1 \times 10^{-2}$ (min^{-1})	7.37	5.77	8.66
R^2	0.984	0.952	0.927
SSE	0.097344	0.003481	1.617984
X^2	0.115473	0.002903	0.553535
Pseudo second order			
$q_{e\ calculated}$ (mg/L)	0.868	0.806	0.6132
K_2 (gmg^{-1}min^{-1})	1.33	1.54	3.02
R^2	1	0.9999	0.999
SSE	0.082369	0.204304	1.077029
X^2	0.094895	0.253479	1.756407
Elovich			
α_{El} (mg/g.min)	0.3037	0.3429	0.3164
β_{El}(g/mg)	4.5055	4.288	3.044
R^2	0.7181	0.7563	0.7642
Intra particle diffusion			
C_1 (mgg^{-1})	0.4949	0.4355	0.4862
K_{diff1}(mgg^{-1}min$^{-1/2}$)	0.2919	0.289	0.323
R_1^2	0.9886	0.9832	0.9946
C_2(mgg^{-1})	1.123	0.931	1.543
K_{diff2}(mgg^{-1}min$^{-1/2}$)	0.003	0.035	0.012
R_2^2	0.879	0.9595	0.5709

Table 4. Thermodynamic parameters for the adsorption of PNP onto RK, CYMK and CHMK.

Adsorbents	ΔH^o (KJ/mol)	ΔS^o (J/mol/K)	ΔG^o (KJ/mol)				
			303	313	323	333	343
RK	0.69	25.51	-7.04	-7.28	-7.54	-7.79	-8.06
CYMK	1.17	26.37	-6.83	-7.09	-7.33	-7.62	-7.88
CHMK	0.31	21.05	-6.07	-6.29	-6.49	-6.7	-6.91

3. Material and Methods

Preparation of adsorbent

Sample collection and Pretreatment

The natural kaolin clay samples were collected from Isale Koko, Ilorin, North Central, Nigeria. Dirts and other unwanted materials were removed. The natural kaolin clay was crushed, grinded; oven dried and sieved using the Tyler screen standard sieve of various sizes.

Purification of raw kaolinite

The natural kaolin clay sample was washed with distilled-deionized water severally. Pulverized washed samples were dispersed in

441

Orbital: Electron. J. Chem. 10 (6): 435-445, 2018

water for four hours. It was subsequently centrifuged at 2400 rpm for one hour. The obtained residue were further treated via heating to 75 °C, in the presence of 1 M sodium bicarbonate and 2 M sodium chloride in order to eliminate inorganic, organic and free cations found in clays inter-layer spaces. The excess carbonate was removed using 0.5 M HCl and several washing eliminated excess chlorides. Organic matters were eliminated via treatment with H_2O_2 (30% v/v) at 70 °C. Purified clay was washed severally with distilled-deionized water, dried at 110 °C and stored in an airtight container for subsequent analysis and usage.

Kaolinite modifications

Cysteine modified kaolinite (CYMK) was prepared following the methods reported by Faghihian and Massoud [28]. A 10 g of treated kaolin clay mineral was suspended in 100 cm^3 0.1 M cysteine solution (pH 4.8), the mixture was agitated for 12 hours, filtered, washed to neutrality and dried at room temperature. The dried cysteine modified kaolinite was stored in air tight containers. Chitosan modified kaolin (CHMK) was prepared following the work of Inyinbor et al. [19].

Adsorbent Characterization

Prepared adsorbents were fully characterized. Elemental composition was determined using X-ray fluorescence (XRF), in order to understand the crystal structure of the adsorbents, a Shimadzu X-Ray Diffractometer, Model 6000 was employed for the X-Ray diffraction (XRD) studies. Functional group analyses as well as morphological studies were done using Fourier Transformed Infrared Spectrometer (FTIR) and Scanning Electron Microscope (SEM) respectively.

Adsorbate preparation

Analytical grade of p-nitrophenol (PNP) was supplied by BDH, 1000 mg/L stock solution of PNP was prepared and subsequent working solutions were prepared from the stock solution by serial dilution.

Equilibrium and kinetics adsorption studies

Batch adsorption studies with respect to effects of pH, adsorbent dosage, initial concentration, contact time, and temperature were carried out. To each 25 cm^3 of 50 mg/L solution of PNP whose pH has been previously varied between pH of 2 and 10, 0.2 g of each of the adsorbents were separately added. Obtained mixtures were agitated for six hours at 30 °C on a thermostated water bath shaker. Residual adsorbent was separated from the solution by filtration and unadsorbed PNP was determined using a Beckman Coulter DU 730 UV/Vis spectrophotometer.

To establish concentration at which driving force is optimal, 25 cm^3 of varying concentrations of PNP (10 to 70 mg/L) with 0.2 g of each of the adsorbents was agitated for six hours on a thermostated water bath shaker operated at 30 °C. Unadsorbed PNP for each concentration was separated and determined as earlier described.

In order to establish the time required to attain equilibrium, a 25 cm^3 solution of 50 mg/L of PNP was agitated with 0.2 g of each of the adsorbent over a period of 6 hours. Samples were withdrawn at intervals, centrifuged and the unadsorbed PNP were analyzed as earlier described.

Temperature effect on the uptake of PNP onto the adsorbents was investigated within the temperature range of 30 and 70 °C. A 25 cm^3 solution of PNP was agitated with 0.2 g of each of the adsorbents while considering optimal pH, concentration, and contact time.

A 25 cm^3 solution of PNP was used against varying dosage of adsorbent (0.1 to 0.5 g) in order to study the effects of increased available adsorption sites. Optimal pH, concentration, contact time and temperature were considered in this study.

Mathematical analysis of adsorption data

Quantity of PNP adsorbed and percentage removal

Equations 1 and 2 were used to calculate the quantity of PNP adsorbed and percentage PNP removed from PNP aqueous solution respectively.

$$q_t = \frac{(C_i - C_t)V}{M} \qquad (1)$$

442

Orbital: Electron. J. Chem. 10 (6): 435-445, 2018

$$\% \; Removal = \frac{(C_i - C_f)}{C_i} \; X \; 100 \qquad (2)$$

where C_i and C_t (mg/L) are the liquid-phase concentrations of the adsorbates at initial and at any time t, respectively. C_f is the final adsorbate concentration (mg/L), V is the volume of the solution (L), and W is the mass of dry adsorbent used (g).

Mathematical modeling of adsorption data

Isothermal modeling

Kaolin and modified kaolin-PNP systems adsorption data were analyzed using the Langmuir [29], Freundlcih [30] and Temkin [31] isotherm models. The Langmuir isotherm models best describes a monolayer adsorption, in which the uptake of pollutants is usually onto a uniform surface. The Freundlich adsorption isotherm describes adsorption onto a multi-surface while the Temkin, which describes heat of adsorption linearly rather than logarithm manner. The Langmuir, Freundlich, and Temkin equations are expressed mathematically by equations 3, 4 and 5. Equation 3a and 5a are the Langmuir dimensionless R_L factor that describes the favourability of adsorption process and Temkin constant b (J/mol) related to the heat of absorption respectively.

$$\frac{C_e}{q_e} = \frac{C_e}{q_{max}} + \frac{1}{q_{max}K_L} \qquad (3)$$

$$R_L = \frac{1}{(1 + K_L C_o)} \qquad (3a)$$

$$\log q_e = \frac{1}{n} \log C_e + \log K_f \quad (4)$$

$$q_e = BlnA + BlnC_e \qquad (5)$$

$$B = \frac{RT}{b} \qquad (5a)$$

where C_e and q_e are concentration of adsorbate in solution at equilibrium measured in mg/L and quantity of PNP adsorbed at equilibrium in mg/g respectively. q_{max} is the maximum monolayer adsorption capacity of adsorbent (mg/g) and K_L is the Langmuir adsorption constant (L/mg). K_f and n are Freundlich constants incorporating the factors affecting the adsorption capacity and adsorption intensity respectively. A (L/g) and B are Temkin isotherm constants, T is the absolute temperature (K) and R is the gas constant (J/mol K).

Kinetics modeling

The pseudo first order kinetic [32] assumes a direct proportion between the rate of change of adsorption and time. Pseudo second order kinetics by Ho and McKay [33], which describes the adsorption process for all concentration and may as well, describes chemisorption process. The Elovich kinetic model [34] best describes adsorption onto heterogeneous surface while the intraparticle diffusion model [35] usually describes the main mechanism of adsorption. The quest for insight into the adsorption mechanism results in a test of the adsorption kinetics data using the pseudo first order, pseudo second order, Elovich and the Weber and Morris intraparticle diffusion model expressed by equations 6, 7, 8 and 9 respectively.

$$\ln(q_e - q_t) = lnq_e - k_1 t \qquad (6)$$

$$\frac{t}{q_t} = \frac{1}{k_2 q_e^2} + \frac{t}{q_e} \qquad (7)$$

$$q_t = \frac{1}{\beta}\ln(\alpha\beta) + \frac{1}{\beta} lnt \qquad (8)$$

$$q_t = k_{diff} t^{1/2} + C \qquad (9)$$

where q_e and q_t are quantity of phenol adsorbed at equilibrium, and at time t (mg/g) respectively, k_1 and k_2 are the Pseudo first order rate constant (min^{-1}) and the Pseudo first order rate constant (g/mg min^{-1}), respectively. α and β are Elovich constants which may explain the chemisorption rate and extent of surface coverage respectively. A single linear profile or a multilayer profile may be obtained for the plot of quantity adsorbed at time t (q_t) against the square root of time (t), this describes stages in adsorption process. C is the boundary layer thickness.

Validation of adsorption kinetics

Validation of kinetics model was not limited to the use of correlation coefficient and calculated quantity adsorbed. Statistical tools such as Sum square of error (SSE) and Chi square (X^2) represented by equations 10 and 11 were also used as validation tools;

$$SSE = \sum_{i=1}^{n} \left(q_{cal} - q_{exp}\right)^2 \qquad (10)$$

$$X^2 = \sum_{i=1}^{n} \frac{(q_{exp} - q_{cal})2}{q_{cal}} \qquad (11)$$

443

Orbital: Electron. J. Chem. 10 (6): 435-445, 2018

Thermodynamic studies

Thermodynamic parameters such as the ΔG^o, ΔH^o and ΔS^o explains feasibility, spontaneity as well as the nature of adsorbate-adsorbent interactions. These parameters were calculated using the mathematical relations 12 and 13;

$$lnK_o = \frac{\Delta S^\circ}{R} - \frac{\Delta H^\circ}{RT} \qquad (12)$$

$$\Delta G^\circ = -RTlnK_o \qquad (13)$$

T is the temperature in Kelvin, R is the gas constant and K_o can be obtained from equilibrium concentration and quantity adsorbed at equilibrium. The values of enthalpy (ΔH^o) and ΔS^o can be obtained from the plot of lnK_o versus 1/T.

4. Conclusions

This study focused on adsorption of PNP onto kaolinite and its modified forms. Various adsorption operational parameters such as the effects of adsorbent dosage, initial dye concentration, contact time, pH, and temperature. Multi surface adsorption occurred in the three adsorption systems and the correlation coefficient of the Temkin isothermal model suggests that some level of adsorbate-adsorbate removal occurred within the adsorption systems. CHMK performed the best in PNP uptake. The prepared adsorbent was stable and increase in temperature up to 243 K did not affect PNP removal across the three systems**.**

References and Notes

[1] Liu, B.; Yang, F.; Zou, Y.; Peng, Y. *J. Chem. Eng.* **2014**, *59*, 1476. [Crossref]

[2] Zhang, L.; Zhang, B.; Wu, T.; Sun, D.; Li, Y. *Colloids Surf. A* **2015**, *484*, 118. [Crossref]

[3] Xue, G.; Gao, M.; Gu, Z.; Luo, Z.; Hu, Z. *Chem. Eng. J.* **2013**, *218*, 223. [Crossref]

[4] Ivančev-Tumbas, I.; Ralph Hobby, R.; Küchle, B.; Panglisch, S.; Gimbel, R. *Water Research* **2008**, *42*, 4117. [Crossref]

[5] Parham, H.; Saeed, S. *J. Chromatogr. A* **2014**, *1336*, 34. [Crossref]

[6] Pandey, S.; Mishra, S. B. *Carbohydr. Polym.* **2014**, *113*, 525. [Crossref]

[7] Huong, P.; Lee, B.; Kim, J.; Lee, C. *Materials and Design* **2016**, *101*, 210. [Crossref]

[8] Ngassa, G. B. P.; Tonlé, I. K.; Ngameni, E. *Talanta* **2016**, *147*, 547. [Crossref]

[9] Víctor-Ortega, M. D.; Martins, R. C.; Gando-Ferreira, L. M.; Quinta-Ferreira, R. M. *Colloids Surf., A* **2017**, *531*, 18. [Crossref]

[10] Inyinbor, A. A.; Adekola, F. A.; Olatunji, G. A. *Water Res. Ind.* **2016**, *15*, 14. [Crossref]

[11] Thue, P. S.; Adebayo, M. A.; Lima, E. C.; Sieliechi, J. M.; Machado, F. M.; Dotto, G. L.; Julio, C. P.; Vaghetti, J. C. P.; Dias, S. L. P. *J. Mol. Liq.* **2016**, *223*, 1067. [Crossref]

[12] Varank, G.; Demir, A.; Yetilmezsoy, K.; Top, S.; Sekman, E.; Bilgili, M. S. *Indian J. Chem. Technol.* **2012**,*19*, 7.

[13] Djebbar, M.; Djafri, Bouchekara, F. M.; Djafri, A. *Appl. Water Sci.* **2012**, *2*, 77.

[14] Agarry, S.; Ogunleye, O. *Turkish J. Eng. Env. Sci.* **2014**, *38*, 11.

[15] Liu, X.; Wang, F.; Bai, S. *Water Sci. Technol.* **2015**, *72*, 2229.

[16] Dhorabe, P. T.; Lataye, D.H.; Ingole, R. S. *Water Sci.Technol.* **2016**, *73*, 955.

[17] Matus, C.; Camú, E.; Villarroel, M.; Ojeda, J.; Baeza, P. *J. Chil. Chem. Soc.* **2016**, *61*, 2898.

[18] Ahmedzeki, N. S.; Rashid, H. A.; Alnaama, A. A.; Alhasani, M. H.; Abdulhussain, Z. *Korean J. Chem. Eng.* **2013**, *30*, 2213.

[19] Inyinbor, A. A.; Adekola, F. A.; Olatunji, G. A. *Appl. Water Sci.* **2017**, *7*, 2297.

[20] Ashour, R. M.; Abdel-Magied, A. F.; Abdel-khalek, A. A.; Helaly, O. S.; Ali, M. M. *J. Env. Chem. Eng.* **2016**, *4*, 3114.

[21] Zheng, W.; Zhou, J.; Zhang, Z.; Chen, L.; Zhang, Z.; Li, Y.; Ma, N., Du, P. *J. Colloid Interface Sci.* **2014**, *432*, 278. [Crossref]

[22] Srinivasan, R. *Adv. Mater. Sci. Eng.* **2011**, *Article ID 872531*, 1. [Crossref]

[23] Inyinbor, A. A.; Adekola, F. A.; Olatunji, G. A. *S. Afr. J. Chem.* **2016**, *69*, 218. [Crossref]

[24] Li, J.; Meng, X.; Hu, C.; Du, J. *Bioresour. Technol.* **2009**, *100*, 1168. [Crossref]

[25] Vaghetti, J. C. P.; Lima, E. C.; Royer, B.; Cunha, B. M.; Cardoso, N. F.; Basil, J. L.; Dias, S. L. P. *J. Hazard. Mater.* **2009**,*162*, 270. [Crossref]

[26] Bello, O. S.; Auta, M.; Ayodele, O. B. *Chem. Ecol.* **2013**, *29*, 58. [Crossref]

[27] Mittal, H.; Mishra, S. B. *Carbohydr. Polym.* **2014**, *101*, 255. [Crossref]

[28] Faghihian, H.; Massoud, N. *J. Serb. Chem. Soc.* **2009**, *74*, 833.

[29] Langmuir, I. *J. Am. Chem. Soc.* **1916,** *38*, 2221. [Crossref]

[30] Freundlich, H. M. F. *Zeitschrift fur Physikalische Chemie* **1906**, *57*, 385.

[31] Temkin, M. I.; Pyzhev, V. *Acta Physiochimica* **1940**, *12*, 327.

[32] Lagergren, S.; Svenska, B. K. *R. Swed. Acad. Sci.Doc, Band* **1898**, *24*, 1.

[33] Ho, Y. S.; McKay, G. *Process Biochem.* **1999**, *34*, 451. [Crossref]

444

Orbital: Electron. J. Chem. 10 (6): 435-445, 2018

[34]   Aharoni, C.; Ungarish, M. *J. Chem. Soc. Farad. Trans.* **1976**, *72*, 265.

[35]   Weber, W. J.; Morris, J. C. *Journal of Sanity Engineering Division of American Society of Civil Engineers* **1963**, *89*, 31.

445

Orbital: Electron. J. Chem. 10 (6): 435-445, 2018